Universidad de Granada

Internship report

Partitioning boundary-layer fluxes into turbulent and non-diffusive components

Gabriela Miranda García

Supervisors: dr. Andrew Kowalski
prof.dr. Jordi Vilà-Guerau de Arellano

18/07/2018

CONTENTS

1. INTRODUCTION

In recent decades the impact of climate change has been remarkable. In 2017, the dominant greenhouse gases (GHG) released into the atmosphere (carbon dioxide, methane and nitrous oxide) reached new record highs. The global growth rate of carbon dioxide has nearly quadrupled since the beginning of the industrial era [1]. Its concentration in the atmosphere has risen from an annual average of 280 ppm in the late 1700's to 401 ppm as measured at Mauna Loa in 2015 [2]. Human activities are the most significant contributor to the total GHG emissions, and have increased 35% worldwide from 1990 to 2010. Distinct forms of energy production and use are the responsible of the majority of world emissions. This leads to serious consequences for the environment including global temperature increase, loss of biodiversity, sea-level rise, extreme climate events, and loss of biodiversity among others. [3]

As a preventive measure to climate change, in 1997 an international agreement was ratified known as the Kyoto Protocol. Linked to the United Nations Framework Convention on Climate Change, the agreement commits its Parties to reduce their GHG emissions. Article 3.3 of the protocol states that the greenhouse gas emissions by sources and removals by sinks shall be reported by each Party in a transparent and verifiable manner and reviewed [4]. Since 1997 the need of identify and quantify carbon dioxide emissions and sinks has increased, expanding the use of the Eddy Covariance (EC) flux towers. The development of tower networks became more important and the propagation of towers from the 1st European network [5] to a global network [6] had encompassed by 2015 more than 750 towers around the world (FLUXNET Website : https://fluxnet.fluxdata.org/sites/historical-site-status/).

Measuring carbon dioxide flux with EC has advantages because it covers a large range of ecosystems, topography and canopy morphology on spatial and temporal scales of km^2 and hours to decades, respectively [7, 8]. The EC technique is preferred worldwide since it is one of the most accurate and direct approaches to measure the exchange of gases. It directly measures the net ecosystem exchange (NEE) that is the difference between gross ecosystem photosynthesis and total ecosystem respiration, and the evapotranspiration, that consist of both plant transpiration and direct evaporation from soil, litter and vegetation surfaces [9]. Although, the EC has limitations as well, since the method is most applicable over flat terrains and with steady environmental conditions [10-12].

Surface-atmosphere exchange is defined in micrometeorology to be purely diffusive in nature and it is related to the covariance between the vertical wind velocity and the concentration of the gas of interest. The EC flux $\mathrm{F_{EC}}$ is expressed as:

$$F_{EC} = \bar{\rho}\overline{w's'} \tag{1}$$

where *w* is the vertical wind velocity and *s* is the mixing ratio or dry mole fraction of the constituent of interest in the air as $\mathrm{CO_2}$ [13]. The upper bar denotes time averaging in a 30min interval and the primes denote fluctuation from the mean.

Two major assumptions are considered to derive (1):

1. Covariances between air density and both the mixing ratio and air velocity are assumed to be negligible (neglecting terms such as $\overline{w}\,\overline{\rho_d's'}$, $\bar{s}\,\overline{\rho_d'w'}$) and $\overline{w'\rho_d's'}$).
2. Mean vertical flow is assumed to be negligible for horizontal homogeneous terrain:

$$\overline{w\rho_d} = 0 \tag{2}$$

where ρ_d is the dry air density. This assumption implies a zero mean vertical wind velocity that is not accurate since heat and humidity can influence the air parcels density near the surface and therefore can result in an upward mean velocity $\overline{w}$ and fluctuations in the constituent's density. For this reason, Webb et al. (1980) derived corrections (hereafter WPL) that are applied to all measurements of fluxes of constituents as CO_2 and that account for heat and humidity effects on the constituent density. The corrections are not necessary when measurements involves sensing of mixing ratio relative to dry air, but they are necessary when sensing the constituent's density [14].

The WPL derivation of the turbulent flux have been accepted in the literature for decades, however it has flaws in the derivation of the mean vertical velocity $\overline{w}$ that need to be re-evaluated. Even though it is not stated explicitly, determining an expression for $\overline{w}$ implies a simple arithmetic averaging:

$$\overline{w} = \frac{1}{N}\sum_{i=1}^{N} w_i \tag{3}$$

This is not in agreement with Reynolds's averaging rules [15] that presents the averaging velocities using the fluid density as a weighting factor [16]:

$$\overline{w} = \frac{\sum_{i=1}^{N} w_i\rho_i}{\sum_{i=1}^{N} \rho_i} \tag{4}$$

An arithmetic averaging for the vertical velocity assumes that every particle in the air contributes equally to the mean vertical velocity. This is not in accordance with conservation principals. Vertical wind velocity expressed in (4) is accurate because it defines a density-weighted average that is in accordance with the law of conservation of linear momentum and that is the true definition of Reynolds's average. This misinterpreted definition can impact the value of a net turbulent flux. Additionally, Kowalski (2017) states that the micrometeorology community has ignored the contribution of the Stefan flow to the total flux of a constituent [17-19]. The net upward momentum in the surface layer is forced by evaporation that induces a pressure gradient force driving winds away from the surface [20]. The Stefan flow is non-diffusive in nature and its velocity is proportional to the total evaporation:

$$\overline{w}_{Stefan} = \frac{E}{\overline{\rho}} \tag{5}$$

The contribution of this flux to the total gas exchange has been underestimated. Considering this flow is crucial since this changes the definition that has been accepted for decades in micrometeorology that the net flux of any gas is driven only by a diffusive process. Kowalski (2017) states that the net flux $F_{net,c}$ of any constituent *c* is the juxtaposition of two types of transport, one of turbulent and diffusive nature $F_{diff,c}$ and another of non-diffusive nature

$F_{non,c}$ [20]. This has an effect on the estimation of the partitioning of NEE and total evapotranspiration.

Furthermore, there is a lack of agreement in the micrometeorology community about the definition of the quantity *s* in the turbulent flow (1) since we can find in the literature definitions as: concentration, mixing ratio, density or simply as a scalar [21]. This inappropriate interpretation leads to confusion in the quantification of the fluxes. Kowalski (2017) suggests the correct quantity to consider is the mass fraction f_c defined as:

$$f_c = \frac{\rho_c}{\rho} \tag{6}$$

where ρ_c is the density of the constituent and ρ is the air density.

We believe that the flaws described previously are the origin of discrepancies in the estimation of fluxes using the EC technique. It has been observed that the EC technique does not match the estimates of net ecosystem productivity produced with ecological methods [22, 23]. Moreover, the EC technique is not able to close the surface energy budget, since it has been observed an underestimation of turbulent fluxes in the order of 20% [24-26]. For this reason, the aim of our study is to apply the corrections stated by Kowalski [15, 20, 21] to improve the estimation of CO_2 and water vapor net fluxes. The corrections can be summarized in the following expression of a net flux:

$$F_{net,c}=F_{non,c}+F_{diff,c}= E f_c + \bar{\rho}\overline{w' f_c'} \tag{7}$$

where F_{non} is the non diffusive flux (Stefan flow) composed by the total evaporation flux *E* and the constituent molar fraction f_c, and F_{diff} is the turbulent flux that considers the fluctuation of a corrected averaged vertical wind velocity and the fluctuation of the constituent molar fraction.

2. MATERIALS AND METHODS

The site study is a wetland located in El Padul (Figure 1) in the province of Granada, southern Spain within the Sierra Nevada National Park (37°00' N, 03°36' W) with an elevation of 744m. The wetland surface is of 3.3 km^2. The dominant plant species is the *Phragmites Australis* or Common Reed. The micro-meteorological station started operating in 2012. The station is called "ES-pdu" in the European Fluxes Database cluster. The tower footprint is close to 0.5 km^2. It is equipped with a sonic anemometer CSAT-3 (CAMPBELL SCIENTIFIC inc., Logan, UT, USA) at 6m that measures wind speed in its three components (*u, v, w*) and temperature with a response of 10 Hz, and an open-path IRGA (Infra Red Gas Analyzer) LI-7500 (Li-Cor; Lincoln, NE, USA) that measures water vapor and carbon dioxide gas densities also at 6m. A net radiometer (NR Lite, Kipp & Zonnen, Delft, Netherlands) located 5 m above the surface together with four heat flux plates (HFP01SC, Hukseflux, Delft, Netherlands) at 8 cm depth, and two pairs of soil temperature probes (TCAV, CSI) at 2 and 6 cm depth are installed parallel to the surface to examine the energy balance. Air temperature and relative humidity are also measured with a thermohygrometer (HMP 45C, CSI) at 5m.

Wetlands are dynamic and natural ecosystems characterized to be areas covered by water permanently or seasonally. Padul is a wetland that is flooded more than half of the year meaning that the rate of evaporation is high. Figure 1.b shows that stagnation of water is observed at the site. This is convenient for our study since we are considering a Stefan flow as a result of evaporation that contributes to the net flux of any constituent. Furthermore, wetland mechanisms can facilitate low cost approach of Kyoto Protocol in lowering net emission of GHGs[27] making it important to accurately measure the exchange of GHG in this ecosystem with the atmosphere.

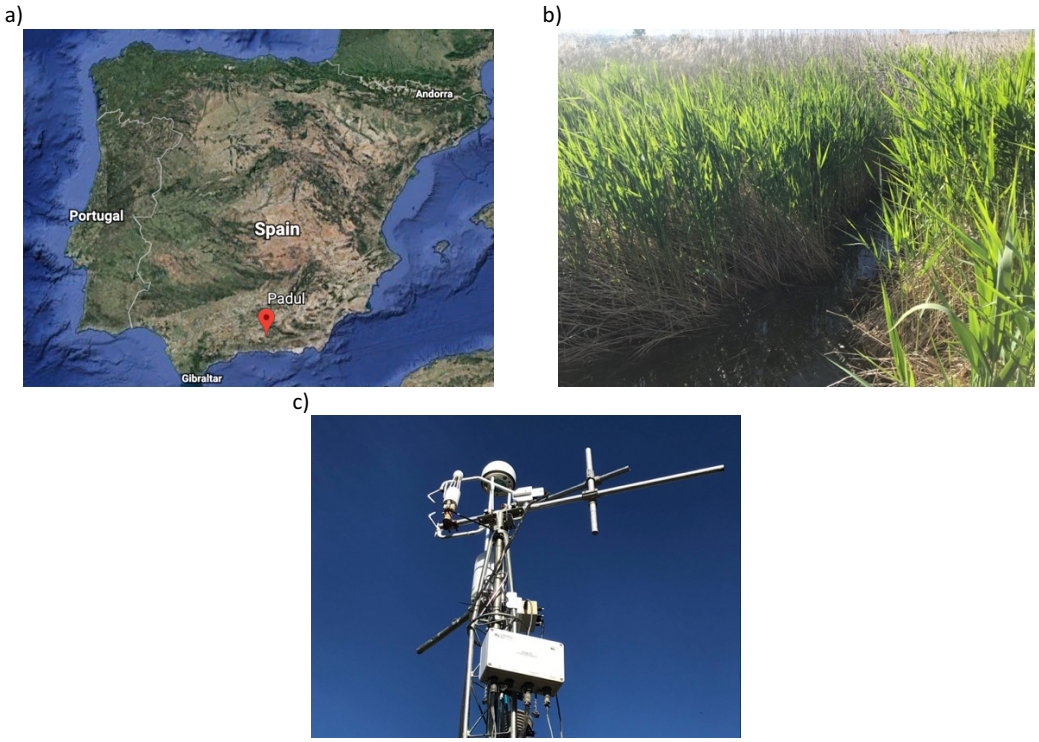

Figure 1. a. Location of Padul marked with a red dot, b. Dominant plant in site: common reed, c. Meteo tower installed at site

Another reason to choose the Padul site is that it is homogeneous meaning it has a dominant type of vegetation over very flat terrain. This offers an advantage in the calculation of net flux.

We used data collected in 2013 and 2018 with measurements of wind speed, temperature, water vapor and carbon dioxide densities. We first processed the raw data with the EddyPro software package [28] in order to remove the spikes and apply the axis rotation for tilt correction. After this process, we obtained two time series, one called *fast*, with same frequency as the raw data (10Hz) and other one called *slow* with data being averaged every 30 min. Table 1 shows a summary of available data.

From measurements with the thermo-hygrometer and barometer we obtained averaged values of $\overline{T}$, water vapor $\bar{e}$ and pressure $\overline{P}$ to calculate and correct the estimation of air density ρ, temperature T and specific humidity q as well as their average and fluctuating terms

necessary for the definition of fluxes. The procedure for this improved estimation of these variables is explained in Appendix I.

Table 1. Available data used for the estimation of surface fluxes

Response	Variable	Instrument
Fast (10 Hz)	U: Wind speed and components (u, v, w) T_s: Temperature	Sonic anemometer
	ρ_v: Water vapor density	IRGA
	ρ_{CO_2}: Carbon dioxide density	
Slow (30min average)	$\overline{P}$: Pressure	Barometer
	$\overline{T}$: Temperature	Thermo-hygrometer
	$\overline{U}$: : Wind speed and components (u, v, w)	Sonic anemometer

A MATLAB© script was developed to treat the data and compute the fluxes applying the corrections proposed by Kowalski (2017). We describe in this section the algorithm used for this study. We also developed a script to compute the fluxes applying the WPL corrections, to be validated against calculations from the EddyPro package. The equations used for these corrections are (24) and (25) of Webb et. al (1980).

We were interested in compare the difference in the fluxes and their components on every season of the year. Thus, we selected one day per season of the year, using the dataset from January to July of 2013 to compute the fluxes. Due to lack of available data for the rest of the year, we used the dataset of 2018 selecting one day per season from August to December.

As mentioned in the introduction, we are interested in the mass fraction of water vapor and CO_2 to determine the total net flux. We use the expression (6) and we observe that for the water vapor the mass fraction is simply the specific humidity (*q)*, and for the CO_2 we defined the mass fraction as:

$$f_{co2} = \frac{\rho_{co2}}{\rho} \tag{8}$$

We calculate the 30min average $\overline{f_c}$ simply as the arithmetic average and the fluctuating term f_c' as the difference between the fast measurements and the average ($f_c - \overline{f_c}$).

We calculated daily fluxes according to Kowalski corrections (7). The Stefan flow was defined by the evaporation flux and the air density as:

$$\overline{w} = \frac{E}{\overline{\rho}} \tag{9}$$

The non-diffusive water vapor flux is defined as:

$$F_{non,v} = \overline{w}\,\overline{\rho_v} = \bar{\rho}\,\overline{w}\,\overline{q} \tag{10}$$

The diffusive water vapor flux is defined as:

$$F_{diff,v} = \frac{1}{N}\sum_{i=1}^{N} \rho\, w'q' \tag{11}$$

The total evaporative flux *E* or $F_{net,H2O}$ is the sum of (10) and (11). Since the total evaporative flux *E* is used for the definition of the vertical wind velocity (9) and this last one is used for the definition of the total evaporative flux we iterated these values until convergence of *E.* The iteration is explained in detail in Appendix I.

The non-diffusive CO_2 flux is defined as:

$$F_{non,CO_2} = \overline{w}\,\overline{\rho_{co_2}} = \overline{\rho}\,\overline{w}\,\overline{f_{CO_2}} = E\,\overline{f_{CO_2}} \tag{12}$$

The diffusive CO_2 flux is defined as:

$$F_{diff,CO_2} = \frac{1}{N}\sum_{i=1}^{N} \rho\, w' {f_{CO_2}}' \tag{13}$$

The net CO_2 flux $F_{net,CO2}$ or Net ecosystem Exchange (NEE) is the sum of (12) and (13).

Finally, the sensible heat flux was also calculated according to the corrections made on the estimation of average temperature, similar to the average of wind speed stated in (4) but using the specific heat ρC_p as a weighting factor (Appendix I). The sensible heat flux is:

$$H = \frac{1}{N}\sum_{i=1}^{N} Cp\ \rho\ w'T' \tag{14}$$

We compared our estimation of the water vapor, carbon dioxide and heat fluxes with the ones including the WPL corrections calculated with our MATLAB© script, which were validated against the results of EddyPro. It is important to mention that we discarded the spectral and lag corrections.

3. RESULTS

In this section we present the net water vapor and carbon dioxide fluxes ($F_{net,H2O}$ and $F_{net,CO2}$) representative of every season (winter, spring and summer of 2013 and autumn of 2018) applying the corrections by Kowalski ($F_{Kowalski}$) and the comparison with the corrections by WPL (F_{WPL}). Positive flux represents mass and energy transfer from the surface into the atmosphere and negative denotes the opposite.

Figure 2 shows the net flux F_{H2O}, its partition into the non-diffusive and the diffusive component and the net flux F_{CO2} corresponding to both methods from 06:00 UTC to 22:00 UTC with the 30min interval of the 25th of May 2013 (spring). We observe in Figure 2.a that both fluxes reach a maximum of 5.68 mmol m^{-2} s^{-1}. Additionally, Figure 2.a shows that there is a negligible difference between the two methods. The maximum difference $F_{Kowalski}$ - F_{WPL} is 0.026 mmol m^{-2} s^{-1}.

In spring, the Stefan velocity $\overline{w}_{Stefan}$ is on the order of tens to over a hundred μms^{-1}. For this day, the range of the Stefan velocity is from 2.947 to 93.95 μms^{-1}. These values are very low compared to the vertical velocity fluctuations *w'* that range from 10^{-3} to 10^{-2} ms^{-1}. This difference is reflected in Figure 2.b that shows the partition of the net flux into non-diffusive and diffusive components. We observe that the magnitude of the non-diffusive is not

significant (note the difference in scales); it represents about 0.8% of the total flux meaning that it is principally diffusive in nature.

Figure 2.c shows there is no considerable difference between the two methods for estimating the net flux F_{CO2}. We observe that both reach a maximum of -9.64 μmol m^{-2} s^{-1} and the maximum difference $F_{Kowalski}$ - F_{WPL} is 0.03 μmol m^{-2} s^{-1}.

The net F_{H2O} flux and the net F_{CO2} flux corresponding to other seasons showed that there is no significant difference between the two methods (Table 2) and that the diffusive component of the net F_{H2O} flux is dominant in the total flux, the same as the results shown in Figure 2. Table 2 shows the summary of these variables for all seasons. As mentioned before we chose the 25th of May 2013 as representative results for spring. For summer we chose the 14th of July 2013, for autumn we selected the 2nd of October, 2018 and for winter we selected the 14th of January 2013. We selected these days because they have more good quality data compared to other days.

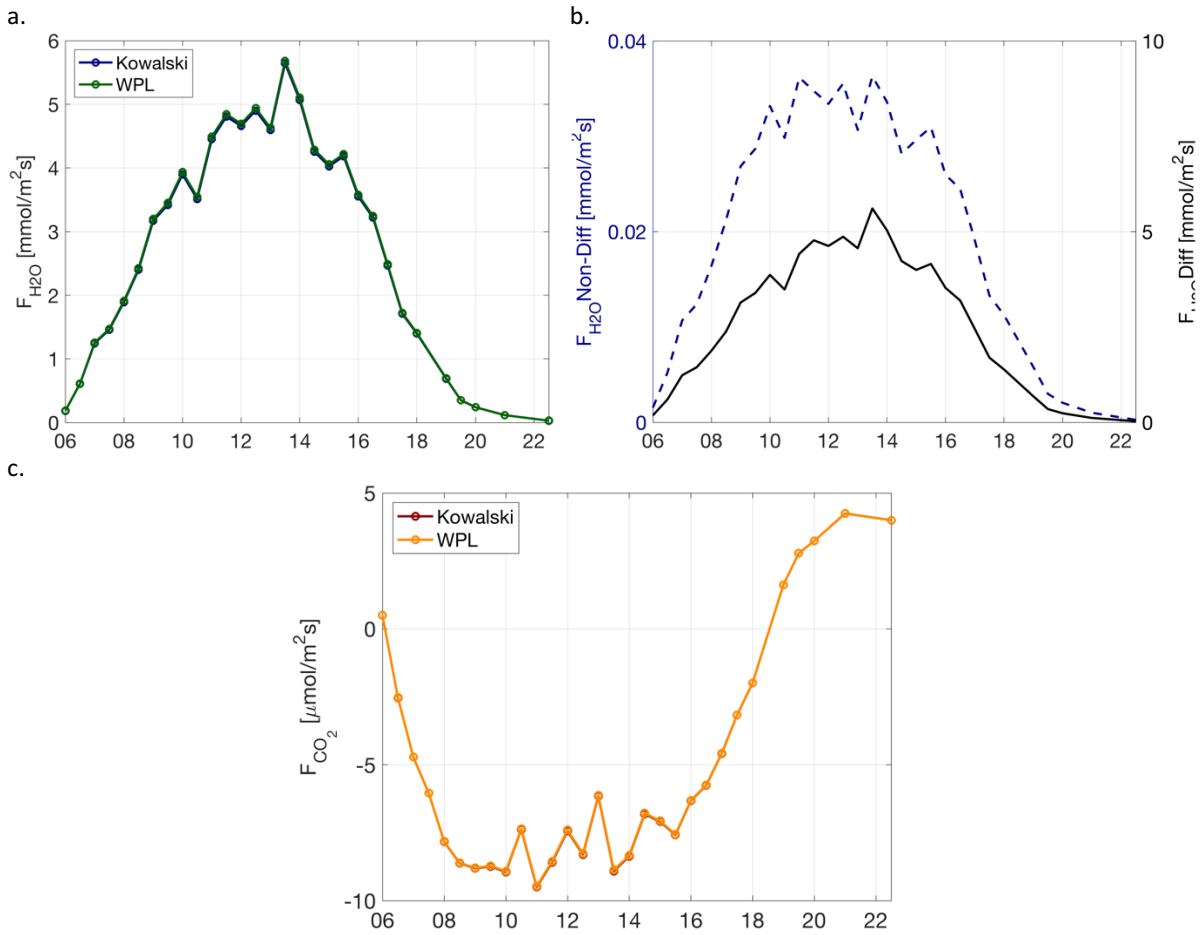

Figure 2. Net F_{H2O} in spring (25th of May 2013) from 06:00 UTC to 22:00 UTC with 30min interval at wetland Padul, Granada. 2.a. Comparison of net F_{H2O} between our methodology (Kowalski) and the WPL corrections (WPL), 2.b. Partition of net F_{H2O} into its components (dashed line corresponds to non-diffusive and solid line to diffusive) according to our methodology., 2.c. Net F_{CO2} in spring.

Table 2. Minimum and maximum values of $\overline{w}_{Stefan}$, average difference between two methods (Kowalski-WPL) for net F_{H2O} and F_{CO2} fluxes

	$\overline{w}_{Stefan}$ [μms^{-1}]	Net F_{H2O} (Kowalski-WPL) [mmol $m^{-2} s^{-1}$]	Net F_{CO2} (Kowalski-WPL) [$\mu mol\ m^{-2} s^{-1}$]
spring	2.947-93.95	0.026	0.016
summer	26.425-160.516	0.019	0.007
autumn	26.626-146.365	0.082	-0.030
winter	6.309-30.157	0.003	0.019

Table 3. Average Diffusive and Non-Diffusive components of F_{H2O} and F_{CO2}

	F_{H2O} Non-Diffusive [mmol $m^{-2} s^{-1}$.]	F_{H2O} Diffusive [mmol $m^{-2} s^{-1}$.]	F_{CO2} Non-Diffusive [$\mu mol\ m^{-2} s^{-1}$.]	F_{CO2} Diffusive [$\mu mol\ m^{-2} s^{-1}$.]
spring	0.024	3.204	0.745	-7.290
summer	0.034	6.503	1.543	-13.728
autumn	0.070	5.276	1.241	-9.237
winter	0.005	1.159	0.278	1.489

Table 3 shows the components of the water vapor and carbon dioxide fluxes. In contrast to the results of F_{H2O} that showed a small contribution of the non-diffusive component to the net flux, when we decomposed the net $\mathbf{F_{CO2}}$ we observed a significant non-diffusive component. For example, in autumn the non-diffusive component amounts to about 15% of the net $\mathbf{F_{CO2}}$ of 7.996 $\mu mol\ m^{-2} s^{-1}$ (downward). Figure 3 shows the net flux, the non-diffusive and diffusive fluxes of $\mathbf{F_{CO2}}$ for all seasons. Because we already showed in Table 2 that the difference between the WPL and Kowalski corrections are not considerable, we only show the result of the net flux that corresponds to our method.

In Figure 3 we observe for all seasons a non-diffusive flux that is positive because the Stefan wind velocity is proportional to the evaporation that is always upward. Only for the day selected in spring (25th of May 2013) we had enough good quality data to observe the components of the flux during nighttime. Carbon dioxide flux is negative during the day and positive at night (after 18:00 UTC in Figure 3.a). It was expected to observe a significant contribution of the non-diffusive component to the net flux when the net flux approaches zero, although Figure 3.a shows that near zero around 19:00 UTC the contribution of this component is not large. Figure 2 depicts a negative diffusive flux for all seasons except for winter when the vegetation is dry and therefore no photosynthesis is observed. As shown in Table 2, the Stefan mean vertical velocity $\overline{w}_{Stefan}$ is higher in summer and autumn (14th July 2013 and 2nd October 2013) leading to higher Non-Diffusive component of the flux as shown in Table 3. Figure 3.d depicts the lowest Non-diffusive flux is observed in winter with a maximum of 0.5 $\mu mol\ m^{-2} s^{-1}$.

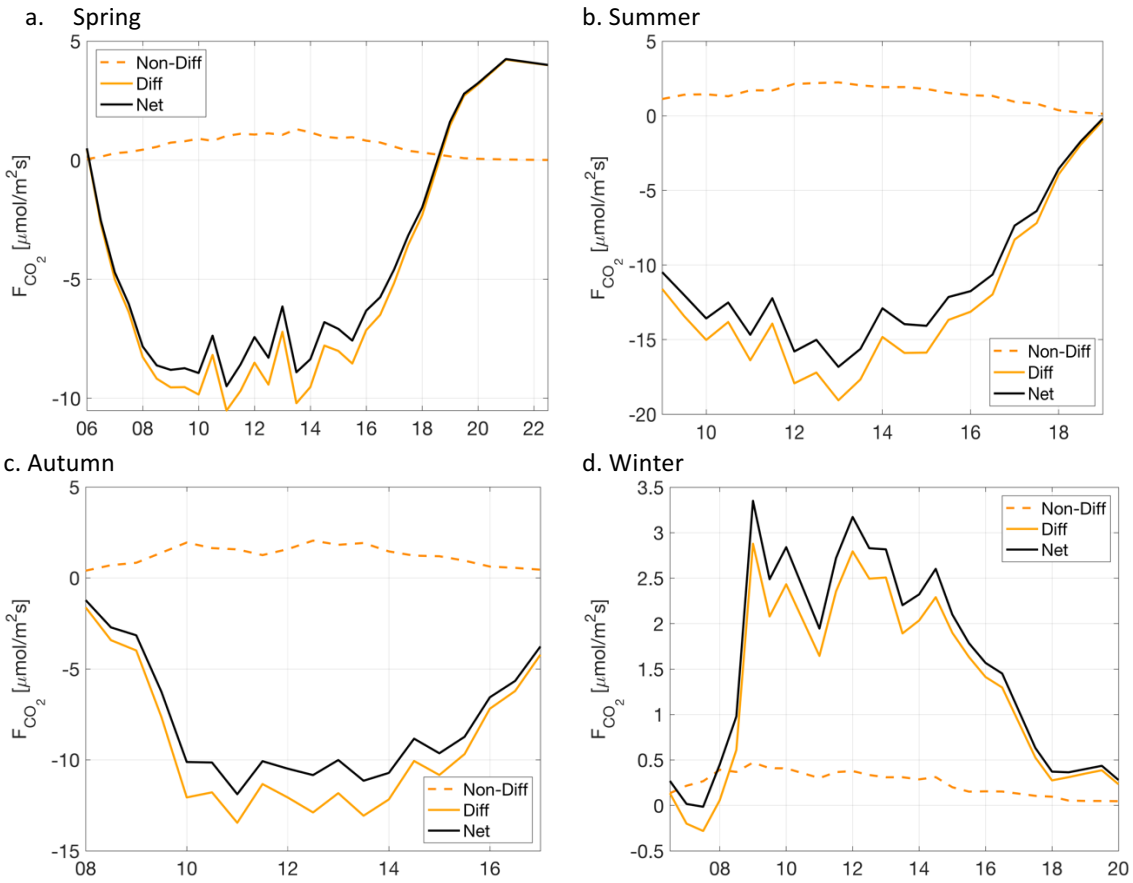

Figure 3. Net F_{CO2} flux and its components in the 30min interval, for every season at wetland Padul,Granada. 3.a. Fluxes for day selected in spring, 3.b Fluxes for day selected in summer, 3.c Fluxes for day selected in autumn and 3.d Fluxes for day selected in winter.

Finally, the results for the sensible heat flux *H* showed that our methodology in which we corrected the definition of temperature averaging considering ρCp as a weighting factor gives values that are very similar to the observed doing an arithmetic average as it is commonly done. We observed these results in all seasons, therefore we only show the result for the 25th of May 2013.

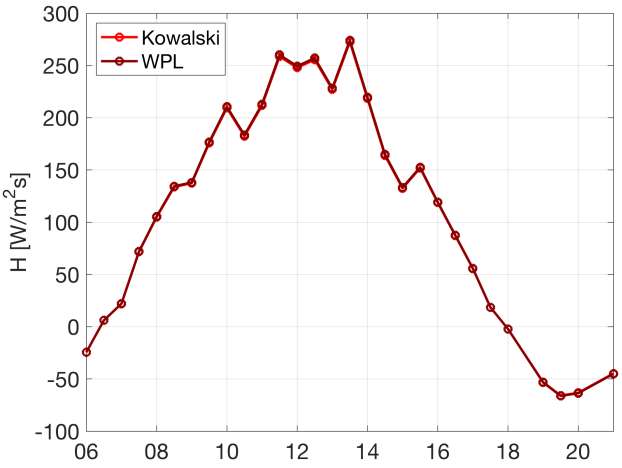

Figure 4. Sensible heat flux in spring (25th of May, 2013) from 10:00 UTC to 18:00 UTC with 30min interval at wetland Padul, Granada. Comparison between the corrections stated in our methodology (Kowalski) and the traditional arithmetic average of temperature as part of the sensible heat flux

4. DISCUSSION

The results of the net F_{CO2} showed that WPL corrections are acceptable since not a significant difference was observed between Kowalski and WPL correction. On the other hand, the results of the carbon dioxide show that the diffusive component of the flux is important and contributes significantly to the net flux. Although the Stefan velocity is measured in μm it generates an upward diffusive flux that reaches 2 μmol m^{-2} s^{-1} in summer and autumn. We did not observe an impact in the net flux for water vapor since this flux is in the order of mmol m^{-2} s^{-1} which is significantly higher to observe a contribution of the Stefan flow.

Figure 2 shows that the net flux of water vapor $F_{net,H2O}$ is dominated by a diffusive process since the magnitude of the Stefan velocity is on average two orders of magnitude lower than the fluctuations of the vertical velocity *w'.* Even though our estimation of net flux considers a diffusive and a non-diffusive process, it is not considerably higher than the net flux with WPL corrections. Since we are prioritizing the physical laws in our methodology for calculating the net flux, we thus conclude that the net fluxes of water vapor with WPL corrections are acceptable.

The sensible heat flux *H* estimated with our methodology compared to the WPL corrections depict that the correction we did on the temperature averaging does not show a considerable improvement to the traditional method. Because the total evaporation and sensible heat flux did not change considerably there is not an improvement in the energy balance. This leads to the conclusion that the traditional method gives acceptable results.

The results in Figure 3 are relevant for the partition of the net ecosystem exchange (NEE) into ecosystem photosynthesis and respiration. In the last decade, approaches have been developed to isolate the components of the total evapotranspiration and the net ecosystem exchange [9, 29-33] due to the need of understanding the role of soil and vegetation in the climate system [31]. However, the partition of net ecosystem exchange into photosynthesis and respiration is based on the flux-variance similarity in which only turbulence is considered to be responsible for the net gas exchange. For this reason, our result depicts that not considering the non-diffusive process in the net CO_2 flux can result in an underestimation of the downward turbulent flux that can be of 11% as in the case of the day selected in summer and consequently an inaccurate estimation of the components of NEE.

Future research can apply the methodology followed in this study but for other two important GHGs: methane (CH_4) and nitrous oxide (N_2O). It is expected that the contribution of a non-diffusive component to net flux of these gases will be higher than that observed for the carbon dioxide. The typical molar flux of CH_4 and N_2O is -2 nmol m^{-2} s^{-1} and 0.02 nmol m^{-2} s^{-1} respectively [20] which means that the magnitude of the Stefan velocity becomes more important for the transport of these constituents.
One key difference that distinguishes fluxes of CH_4 and N_2O from those of CO_2 is that the latter tends to be strongly bi-directional over the diurnal cycle while for the N_2O tends to be upward and for the CH_4 emissions and uptake change between sites and seasons instead of following a diurnal cycle [34]. Therefore, it is more probable that applying our method to the estimation of N_2O can improve results.

5. CONCLUSION

The aim of our study was to apply the corrections stated by Kowalski in order to improve the estimation of CO_2 and water vapor fluxes. We compared the water vapor, carbon dioxide and heat fluxes with the ones that consider the WPL corrections.

Since the results of total evaporation and sensible heat flux did not change considerably there is not an improvement in the energy balance. This leads to the conclusion that the traditional method gives acceptable results despite the flaws in fluxes estimated with WPL corrections.

However, we observed that the diffusive component of the CO_2 is relevant in determining the partition of the net ecosystem exchange (NEE) into ecosystem photosynthesis and respiration. Our result depicts that not considering the non-diffusive process in the net CO_2 flux can result in an underestimation of downward turbulent flux and overestimation of the upward turbulent flux and consequently an inaccurate estimation of the components of NEE.

REFERENCES

1. Blunden, J., et al., *State of the Climate in 2017.* Bulletin of the Amererican Meteorological Society, 2018. **99**(8).
2. Stocker, T.F., et al., *Climate change 2013: The physical science basis*. 2013, Cambridge University Press Cambridge.
3. Rocha, M., et al., *Historical Responsibility for Climate Change–from countries emissions to contribution to temperature increase*. 2015, Available at:[Accessed May 5, 2017].
4. Breidenich, C., et al., *The Kyoto protocol to the United Nations framework convention on climate change.* American Journal of International Law, 1998. **92**(2): p. 315-331.
5. Aubinet, M., et al., *Estimates of the annual net carbon and water exchange of forests: the EUROFLUX methodology*, in *Advances in ecological research*. 1999, Elsevier. p. 113-175.
6. Baldocchi, D., et al., *FLUXNET: A new tool to study the temporal and spatial variability of ecosystem-scale carbon dioxide, water vapor, and energy flux densities.* Bulletin of the American Meteorological Society, 2001. **82**(11): p. 2415-2434.
7. Haslwanter, A., A. Hammerle, and G. Wohlfahrt, *Open-path vs. closed-path eddy covariance measurements of the net ecosystem carbon dioxide and water vapour exchange: A long-term perspective.* Agricultural and forest meteorology, 2009. **149**(2): p. 291-302.
8. Baldocchi, D.D., *Assessing the eddy covariance technique for evaluating carbon dioxide exchange rates of ecosystems: past, present and future.* Global change biology, 2003. **9**(4): p. 479-492.
9. Scanlon, T.M. and W.P. Kustas, *Partitioning evapotranspiration using an eddy covariance-based technique: Improved assessment of soil moisture and land–atmosphere exchange dynamics.* Vadose Zone Journal, 2012. **11**(3).
10. Foken, T. and B. Wichura, *Tools for quality assessment of surface-based flux measurements.* Agricultural and forest meteorology, 1996. **78**(1-2): p. 83-105.
11. Massman, W. and X. Lee, *Eddy covariance flux corrections and uncertainties in long-term studies of carbon and energy exchanges.* Agricultural and Forest Meteorology, 2002. **113**(1-4): p. 121-144.
12. Moncrieff, J., Y. Malhi, and R. Leuning, *The propagation of errors in long-term measurements of land-atmosphere fluxes of carbon and water.* Global change biology, 1996. **2**(3): p. 231-240.
13. Burba, G., *Eddy covariance method for scientific, industrial, agricultural and regulatory applications: A field book on measuring ecosystem gas exchange and areal emission rates*. 2013: LI-Cor Biosciences.
14. Webb, E.K., G.I. Pearman, and R. Leuning, *Correction of flux measurements for density effects due to heat and water vapour transfer.* Quarterly Journal of the Royal Meteorological Society, 1980. **106**(447): p. 85-100.
15. Kowalski, A.S., *Exact averaging of atmospheric state and flow variables.* Journal of the Atmospheric Sciences, 2012. **69**(5): p. 1750-1757.
16. Reynolds, O., *IV. On the dynamical theory of incompressible viscous fluids and the determination of the criterion.* Philosophical transactions of the royal society of london.(a.), 1895(186): p. 123-164.

17. Gale, J., *Availability of carbon dioxide for photosynthesis at high altitudes: theoretical considerations.* Ecology, 1972. **53**(3): p. 494-497.
18. Bird, R.B., W.E. Stewart, and E.N. Lightfoot, *Transport phenomena*. 2007: John Wiley & Sons.
19. Lienhard, J.H., *A heat transfer textbook*. 2011: Courier Corporation.
20. Kowalski, A.S., *The boundary condition for vertical velocity and its interdependence with surface gas exchange.* Atmospheric Chemistry and Physics, 2017. **17**(13): p. 8177-8187.
21. Kowalski, A.S. and P. Serrano-Ortiz, *On the relationship between the eddy covariance, the turbulent flux, and surface exchange for a trace gas such as CO 2.* Boundary-layer meteorology, 2007. **124**(2): p. 129-141.
22. Keller, M., et al., *If a tree falls in the forest….* Science, 1996. **273**(5272): p. 201-201.
23. Piovesan, G. and J. Adams, *Carbon balance gradient in European forests: interpreting EUROFLUX.* Journal of Vegetation Science, 2000. **11**(6): p. 923-926.
24. Leuning, R., et al., *Effects of heat and water vapor transport on eddy covariance measurement of CO 2 fluxes.* Boundary-Layer Meteorology, 1982. **23**(2): p. 209-222.
25. Stoy, P.C., et al., *A data-driven analysis of energy balance closure across FLUXNET research sites: The role of landscape scale heterogeneity.* Agricultural and forest meteorology, 2013. **171**: p. 137-152.
26. Wilson, K., et al., *Energy balance closure at FLUXNET sites.* Agricultural and Forest Meteorology, 2002. **113**(1-4): p. 223-243.
27. Adhikari, S., R.M. Bajracharaya, and B.K. Sitaula, *A review of carbon dynamics and sequestration in wetlands.* Journal of Wetlands Ecology, 2009: p. 42-46.
28. Biosciences, L., *EddyPro software instruction manual.* LI-COR Inc., Lincoln, Nebraska, USA, 2017.
29. Skaggs, T., et al., *Fluxpart: Open source software for partitioning carbon dioxide and water vapor fluxes.* Agricultural and forest meteorology, 2018. **253**: p. 218-224.
30. Gilmanov, T., et al., *Partitioning European grassland net ecosystem CO2 exchange into gross primary productivity and ecosystem respiration using light response function analysis.* Agriculture, ecosystems & environment, 2007. **121**(1-2): p. 93-120.
31. Klosterhalfen, A., et al., *Source partitioning of H 2 O and CO 2 fluxes based on high-frequency eddy covariance data: a comparison between study sites.* Biogeosciences, 2019. **16**(6): p. 1111-1132.
32. Stoy, P.C., et al., *An evaluation of models for partitioning eddy covariance-measured net ecosystem exchange into photosynthesis and respiration.* Agricultural and Forest Meteorology, 2006. **141**(1): p. 2-18.
33. Wang, L., et al., *Partitioning evapotranspiration across gradients of woody plant cover: Assessment of a stable isotope technique.* Geophysical Research Letters, 2010. **37**(9).
34. Nemitz, E., et al., *Standardisation of eddy-covariance flux measurements of methane and nitrous oxide.* International agrophysics, 2018. **32**(4): p. 517-549.

APPENDIX I

Re-composition of key state variables and iteration of water vapor flux

Here we present the process we followed to improve the estimation of air density, temperature and specific humidity. These variables were important to define as part of the accurate definition of net fluxes.

Variables hereafter with over-bars denote they are 30-min averaged. We discarded fast fluctuations of pressure *P*.

From measurements with the thermo-hygrometer and barometer we obtained $\bar{T}$, $\bar{e}$ (water vapor pressure) and $\bar{P}$ to calculate and correct the estimation of air density ρ, temperature T and specific humidity q.

$$\overline{\rho_{dry}} = \frac{\bar{P} - \bar{e}}{R_{dry}\bar{T}}$$

with R_{dry} = 287 J kg^{-1} K^{-1}. The averaged humid air was calculated as:

$$\overline{\rho_v} = \frac{\bar{e}}{(R_v\bar{T})}$$

with R_v=462 J kg^{-1} K^{-1}.

The averaged air density was defined as the sum of these two: $\bar{\rho} = \overline{\rho_d} + \overline{\rho_v}$.

The *fast* measurement of air density was corrected to account for air density fluctuations. First, we did an iteration process. The initial assumption was that the temperature T and the virtual temperature T_v corresponded to the one measured by the CSAT-3 ($T = T_s$; $T_v = T_s$).

With these values, we calculated the vapor pressure, the specific humidity and the air density. This is followed by a correction of T and T_v in order to have a more accurate value. The iteration is as follows:

1. Vapor pressure $e = \rho_v R_v T$
2. Specific humidity $q = 0.622\frac{e}{\bar{p}}$ (vapor mass fraction, f_v)
3. Air density $\rho = \frac{\bar{P}}{(R_d T_v)}$
4. More accurate $T = \frac{T_s}{1+0.51q}$
5. More accurate $T_v = T(1 + 0.61q)$
6. Iterate 1 to 5 until convergence of *T*

The iteration improves the value of the temperature but also the value of air density. Afterwards, we decomposed the air density into its average and turbulent components as follows:

$$\rho = \bar{\rho} + \rho'$$

$$\bar{\rho} = \frac{1}{N}\sum_{i=1}^{N} \rho$$

$$\rho' = \rho - \bar{\rho}$$

For the specific humidity *q,* we decomposed it as mean $\bar{q} = \frac{\overline{\rho_v}}{\bar{\rho}}$ and perturbations $q' = q - \bar{q}$.
In order to re-compose *q* we defined:

$$\bar{q} = 0.622\frac{\bar{e}}{\bar{p}}$$

To finally use the expression:

$$q = \bar{q} + q'$$

In the case of temperature, as mentioned in the introduction, the average for this variable has ben calculated incorrectly since a weighting factor is necessary since temperature is an intensive scalar. The correct temperature average has as weighting factor the product of the air density and the specific heat C_p
The specific heat for humid air is calculated as:

$$C_p = \bar{C}_{p,dry}(1 + 0.84q);\ \bar{C}_{p,dry} = 1005\ \text{J kg}^{-1}\ \text{K}^{-1}$$

Average $\overline{T}$ is expressed as

$$\overline{T} = \frac{\sum_{i=1}^{N} \rho C_p T}{\sum_{i=1}^{N} \rho C_p}$$

The perturbations are calculated as $T' = T - \overline{T}$.

In the Methodology section we stated that an iteration was made to calculate the total water vapor flux. For this iteration, the initial estimate of *E* was defined as the one calculated applying the WPL corrections:

1. Stephan flow velocity $\overline{w} = \frac{E}{\bar{\rho}}$
2. Non-diffusive flux $F_{v,n} = \overline{w}\ \overline{\rho_v} = \bar{\rho}\ \overline{w}\ \bar{q}$
3. Diffusive flux $F_{v,d} = \frac{1}{N}\sum_{i=1}^{N} \rho\ w'q'$
4. Evaporative flux $E = F_{v,n} + F_{v,d}$
5. Iterate with new *E* until convergence